

# Surface-Modified Nanotube Anodes for High Performance Organic Light-Emitting Diode

Eric C-W. Ou,<sup>§,†,\*</sup> Liangbing Hu,<sup>§,†,\*</sup> Gan Ching Ruey Raymond,<sup>†</sup> Ong Kian Soo,<sup>†</sup> Jisheng Pan,<sup>†</sup> Zhang Zheng,<sup>†</sup> Youngbae Park,<sup>‡</sup> David Hecht,<sup>‡</sup> Glen Irvin,<sup>‡</sup> Paul Drzaic,<sup>‡</sup> and George Gruner<sup>\*,†</sup>

<sup>†</sup>Institute of Materials Research and Engineering, 3 Research Link, 117602, Singapore, and <sup>‡</sup>Unidym Inc., 1430 O'Brien Drive, Menlo Park, California, 94025. <sup>§</sup>These authors have contributed equally to this work.

**ABSTRACT** In this work, we reported high performance OLED devices with transparent and conductive carbon nanotube anodes after modification. The modifications include IMRE proprietary PEDOT:PSS composite top coating (PS<sup>C</sup>), concentrated HNO<sub>3</sub> acid soaking, and polymer encapsulation. For PS<sup>C</sup>-modified nanotube thin film anode, we achieved maximum luminescence of ~9000 cd/m<sup>2</sup>, close to ITO-based OLED device performance, and high efficiency of ~10 cd/A, similar with ITO-based OLED device. The performance is approximately 30 to 450 times better than that achieved for OLED devices using CNT anodes by others. In addition, we also investigate the mechanical property, work function, sheet resistance, and surface morphology of modified carbon nanotube thin-film anodes.

**KEYWORDS:** organic light-emitting diodes · carbon nanotubes · surface modification · roughness · PEDOT:PSS

Carbon nanotube (CNT) thin films have found exciting applications.<sup>1–4</sup> The excellent electrical and thermal properties coupled with exceptional mechanical strength and flexibility makes them suitable in organic light-emitting diodes (OLED),<sup>5–7</sup> organic solar cells,<sup>8,9</sup> biomedical,<sup>10</sup> extreme strength composite materials,<sup>11,12</sup> printed electronics,<sup>13,14</sup> and textiles.<sup>15</sup> There is great interest in replacing the conventional indium tin oxide anode for large area electrode use in flexible light emitting displays due to the brittleness of ITO as it cracks easily under stress or bending. In addition, indium is a rare earth metal with stringent supply, so CNTs present an excellent choice to replace ITO as carbon is one of the most abundant element and many methods of synthesizing a large amount of CNT have been found or under research.<sup>16,17</sup> The use of CNT thin film as anodes for OLED is attracting great interest due to their flexibility and work function (4.7–5.2 eV),<sup>18,19</sup> as well as their resistance to various chemicals used during wet processing of OLEDs.

However, there are some challenges to overcome before they can be used com-

mercially as OLED anode material. The roughness of CNT-coated films presents a problem as this results in nonuniform hole injection into the adjacent organic layer. This inherently reduces the lifetime of the device. Because of the large aspect ratio of CNTs, tubes protruding perpendicular to the surface can easily cause a tremendous local electrical field and subsequently cause the shorting of devices.<sup>20</sup> Planarization layers have been proposed to address the roughness of the CNT films and enhancing the conductivity of CNT with little or no loss in the transmittance. Inkjet and spin-coated PEDOT:PSS were reportedly used as planarization for a CNT surface; however, previous formulations tend to result in higher resistance of the CNT films. Ink Jet printed PEDOT:PSS and CNT composition typically tend to have high sheet resistance of about 1000 Ω/sq.<sup>21</sup> The use of PEDOT:PSS and methanol is effective in reducing the roughness of single walled nanotubes substrates, but the light efficiency of 1–2 cd/A is lower than conventional ITO-based displays.<sup>22</sup> Parylene C and thionyl chloride give lower roughness but do not help in decreasing the resistance.<sup>5,23</sup>

In this paper, we modify the surface of nanotube thin film with PS<sup>C</sup>, HNO<sub>3</sub> treatment, and polymer coating, and we investigate the impact of these modifications on device performance. In particular, we investigate in detail the effect of an IMRE proprietary PEDOT:PSS composite formulation (PS<sup>C</sup>) on CNT thin films morphology, mechanical property, work function, sheet resistance, and OLED device performance. Modification of CNT thin film anode greatly improved the OLED device performance, and holds great promise for flexible displays using CNT thin-film electrodes. The picture

\*Address correspondence to ggruner@unidym.com, lhu@unidym.com, eric-ou@imre.a-star.edu.sg.

Received for review January 30, 2009 and accepted June 30, 2009.

Published online July 9, 2009.  
10.1021/nn900406n CCC: \$40.75

© 2009 American Chemical Society

and device structure of a working OLED device are shown in Figure 1. The CNT films with and without PS<sup>C</sup> modification were initially subjected to a 10000 cycle bending to determine their mechanical flexibility properties for OLED application; negligible change in sheet resistance was observed after bending (Table 1). This proves that our PS<sup>C</sup> solution is fully compatible with the CNT network layer in contrast to another PEDOT:PSS/CNT/PET formulation reported by Wang et al.,<sup>24</sup> which shows an increase of nearly 10% after only 1600 bending cycles. We also observed that PS<sup>C</sup> composite solution coated onto CNT/PEN samples has better bending resistance than PS<sup>C</sup> coated onto CNT/PET samples when comparing samples 3 and 5. Indium tin oxide (ITO) bending results on PET (Table 1, sample 7) shows that ITO is highly unsuitable as an electrode for flexible substrates owing to drastic increase in sheet resistance by 217% after a 10000 bending cycle test.

Surface roughness of electrodes is critical for their applications in OLED devices and normally 1–2 nm roughness is required for uniform charge injection and high efficiency. Because of their intrinsic morphology, CNT thin films have high surface roughness, in the range of 9–11 nm.<sup>22</sup> From the AFM study shown (Table 2), the PS<sup>C</sup> modification layer clearly decreases the surface roughness of CNT films. Table 3 summarizes the surface roughness change after PS<sup>C</sup> modifications for different cases. It is clear that the morphology of the rough CNT surface has been drastically smoothed by the PS<sup>C</sup>. For example, the CNT film on PEN substrate has a surface roughness of 14.55 nm. After the PS<sup>C</sup> surface modification, the surface roughness is 6.0 nm. A 5 nm polymer top coating was used to improve the adhesion of CNT thin film on the substrate. The data show that 5 nm polymer-coated CNT films have even larger smoothing effect after PS<sup>C</sup>. The surface roughness decreases to 4.6 nm which indicates that the polymer helps the wetting and PS<sup>C</sup> onto CNT films.

Sheet resistance of a transparent anode needs to be low enough for large scale OLED device application. Currently, typical sheet resistance of 80% transparent CNT thin film is 150–1000 ohms, depending on

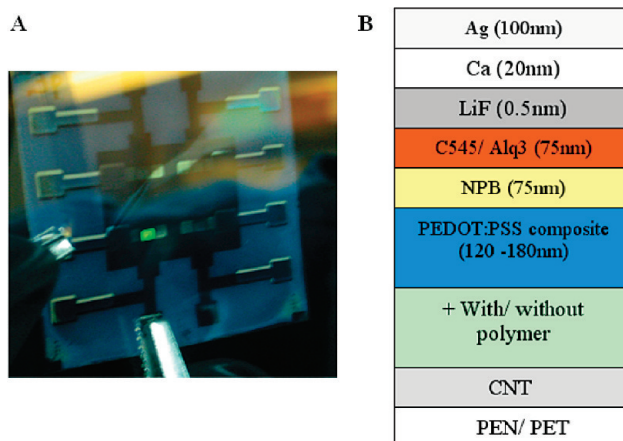


Figure 1. (A) Photograph of working OLED device and (B) diagram showing the layers in the OLED device. Some samples were coated with polymer top coating and some samples were not.

the CNT quality and film fabrication details. Such high sheet resistance is not acceptable for scaled OLED application. Continued improvement of the sheet conductance of CNT thin films is needed. Here we demonstrate that PEDOT:PSS composite (PS<sup>C</sup>) layer modification on CNT thin film decreases the sheet resistance by effectively providing double-layer conduction paths. Spin coating a high conductive and planarization layer from a PS<sup>C</sup> solution onto a PEN substrate yields a sheet resistance of 310.5 Ω/sq; when such a conductive layer is coated on top of CNT thin film, the final sheet resistance is described by the formula

$$R_3 = \frac{R_1 R_2}{R_1 + R_2}$$

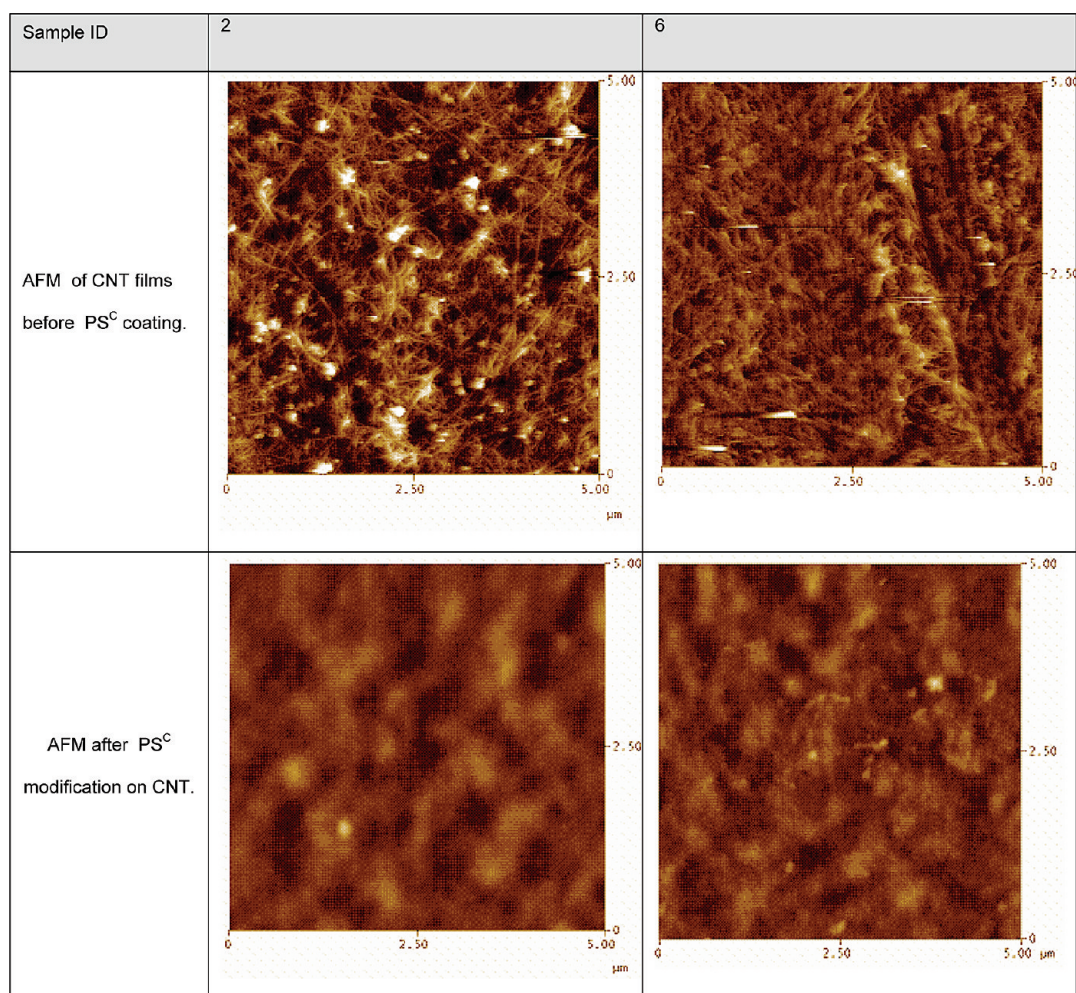
where  $R_1$  and  $R_2$  are the sheet resistances of PS<sup>C</sup> and CNT film, respectively. From Table 4, the measured sheet resistance data matches well with the calculated sheet resistance data using the double layer formula. This indicates that there is no doping effect from PS<sup>C</sup> on CNT films. PS<sup>C</sup> modification decreases the sheet resistance of CNT films by 32.6% and 41.8% for two undoped films and by 4.0% for doped films. The addition of PS<sup>C</sup> layer on sample 6 hardly shows any decrease in sheet resistance; this could be due to some HNO<sub>3</sub> being

TABLE 1. Mechanical Bending Test of Modified CNT Films on PET or PEN and ITO. The Samples Were Subjected to 10000 Cycles Bending with Curvature Radius of 12.5 mm and Frequency of 1 Cycle per Second

sample ID	description	average sheet resistance before bending (Ω/sq)	average sheet resistance after bending (Ω/sq)	change in sheet resistance
1 <sup>a</sup>	PEN/PS <sup>C</sup>	310.5	310.5	0.0%
2	PEN/CNT/PS <sup>C</sup>	102.9	104.7	+1.75%
3	PEN/CNT/5 nm polymer/PS <sup>C</sup>	116.1	116.1	0.0%
4	PET/CNT/PS <sup>C</sup>	163.6	165.2	+0.9%
5	PET/CNT/5 nm polymer/PS <sup>C</sup>	150.2	154.2	+6.01%
6	PET/Doped CNT/PS <sup>C</sup>	135.5	137.6	+1.55%
7	ITO on PET	36.0	78.2	+217%

<sup>a</sup>PEDOT:PSS composite solution (PS<sup>C</sup>) was spin coated on a PEN substrate without any CNT and the average sheet resistance of the film was measured before and after the bending test.

**TABLE 2. AFM Images for Different CNT Films with PS<sup>C</sup> Surface Modification. The Sample IDs Are the Same as Those for Bending Test**



dissolved by the PS<sup>C</sup> solution and evaporated when baked in the oven. We noted that the sheet resistance of HNO<sub>3</sub>-doped CNT is increased after dipping in distilled water, thus explaining the low sheet resistance changes of sample 6 due to the water-based PS<sup>C</sup> layer. The observation that HNO<sub>3</sub>-doped CNT films are unstable in air, water, and thermal loading is supported by Jackson *et al.*<sup>25</sup> Jackson *et al.* demonstrated that a 30% increase in sheet resistance was seen for the

HNO<sub>3</sub>-doped CNT films after 240 h in air and room temperature. Hence, the effect of HNO<sub>3</sub> is considerably being diminished in this aspect. Encapsulating with a thin layer of PEDOT:PSS helps to better preserve the integrity of the HNO<sub>3</sub> dopant used for metallizing semiconducting CNT. The sheet resistance remained stable after 240 h; however, it showed an initial 5% increase on encapsulation with a normal PEDOT:PSS layer. (Table 4)

High work function is critical for a transparent electrode as anode in OLED applications, and the higher work function of an anode is better for hole injection. Theoretical and experiment data have confirmed that the work function of a CNT thin film is in the range of 4.7–5.2 eV.<sup>18,19,26</sup> Therefore a transparent CNT film is a potential candidate for use as an anode in OLED and OPV devices. Conductive PEDOT has been actively developed as transparent anode material because of its high work function (5.0 eV).<sup>9</sup> Here we investigate the CNT film work function change after PS<sup>C</sup> modification. We found, using UPS, that the work function of the CNT films increases by 0.2 eV after PS<sup>C</sup> modification. The increase is not significant which indicates CNT films have

**TABLE 3. Surface Roughness Change of CNT Films before and after PS<sup>C</sup> Modification. The Initial Roughness Data Are for Samples before PS<sup>C</sup> Modifications and the Final Roughness Data Are for Samples after PS<sup>C</sup> Modifications**

sample	description	initial roughness (nm)	final roughness after spin coated with PS <sup>C</sup> (nm)
2	PEN/CNT/PS <sup>C</sup>	14.55	6.0
3	PEN/CNT/5 nm polymer/PS <sup>C</sup>	14.65	4.6
4	PET/CNT/PS <sup>C</sup>	9.3	5.9
5	PET/CNT/5 nm polymer/PS <sup>C</sup>	9.72	5.2
6	PET/Doped CNT/PS <sup>C</sup>	10.85	6.0

**TABLE 4. Average Sheet Resistance of CNT Films before and after PS<sup>C</sup> Modifications and Comparison of Measured and Calculated Data with Double Layer Formula**

sample ID	description	as-is CNT ( $\Omega/\text{sq}$ ), $R_1$	calculated $R_s$ with PEDOT ( $\Omega/\text{sq}$ )	measured $R_s$ with PEDOT ( $\Omega/\text{sq}$ )	% change in measured $R_s$ after PEDOT
2	PEN/CNT/PS <sup>C</sup>	152.7	102.3	102.9	-32.6
4	PET/CNT/PS <sup>C</sup>	281.2	147.6	163.6	-41.8
6	PET/doped CNT/PS <sup>C</sup>	141.1	97.1	135.5	-4.0
Jackson <sup>25</sup>	glass/doped CNT/PEDOT:PSS	140.0		147.0	+5%

very similar work function with the PEDOT:PSS composite layer. We also found 0.13 eV increase after HNO<sub>3</sub> doping and no change after 5 nm polymer top coating on transparent CNT films.

Next we discuss the OLED device performance, with the focus on performance comparison for devices with or without PS<sup>C</sup> layer, with or without HNO<sub>3</sub> treatment, and with or without 5 nm polymer top coating. Prior to using PS<sup>C</sup> layer modification, the turn on voltage was about 20 V for the CNT thin-film electrode on both PEN and PET substrates. The luminescence was very low and the diodes failed quickly. The diode was too short-lived for any characterization. The poor performance of transparent CNT film as anode is mainly due to the rough surface structure. A 14–15 nm surface roughness of CNT thin film is too much if one considers the thickness of the active layer is in the range of 100 nm. There is a high possibility of protruding nanotubes, which generate an extremely high local electrical field. This concentrated field can cause local device failure, which eventually propagates to the entire device. High surface roughness of nanotube thin films prevents it being used as an anode by itself in large scale devices; modification or other type of double layer structures have to be incorporated to smooth out the surface roughness. Normally spin coating 120–180 nm conductive material (as in this study) or sputtering other conductive oxide can smooth the surface roughness.<sup>27</sup> As shown in Figure 2A, the luminescence performance of the PS<sup>C</sup>-solution-coated PEN samples exhibit typical light emitting diodes characteristics. The PS<sup>C</sup> on PEN shows a maximum luminescence of about 2000 cd/m<sup>2</sup> at 20 V and efficiency ranging about 4 cd/A. It is clear from Figure 2 that the performance for PS<sup>C</sup>-modified transparent CNT thin film shows much better performance than PS<sup>C</sup> only devices. One explanation would be due to the lower sheet resistance of PS<sup>C</sup>-modified CNT anode (102.9  $\Omega/\text{sq}$ ) over PS<sup>C</sup> itself (310.5  $\Omega/\text{sq}$ ).

Doping has been proven as an efficient way to improve the conductivity of transparent CNT thin films.<sup>28,29</sup> Meanwhile, it has been proven that doping could be used to tune the work function of a CNT thin film anode which would change the device performance where the CNT thin film anode is used. We report also in this work that HNO<sub>3</sub> not only increases the work function of CNT thin film by approximately 0.13 eV but also decreases the sheet resistance by approximately 50%, from 282.0  $\Omega/\text{sq}$  to 141.1  $\Omega/\text{sq}$ . Figure 3

shows the performance comparison for a device with and without HNO<sub>3</sub> doping. We see clearly the doped device shows higher light luminance, which may be mainly due to the sheet resistance decrease after HNO<sub>3</sub> doping. However, we did not see a significant reduction of turn-on voltage after HNO<sub>3</sub> doping, which may be due to the insignificance of the work function change, only about 0.13 eV, or due to the dissipation of the HNO<sub>3</sub> molecule during device operation. The increase in work function after HNO<sub>3</sub> doping is evident in the paper of Jackson *et al.*<sup>25</sup> Work function modification with other materials such as salts could be more stable to show the device turn-on voltage shift after a certain amount of time of device operation.

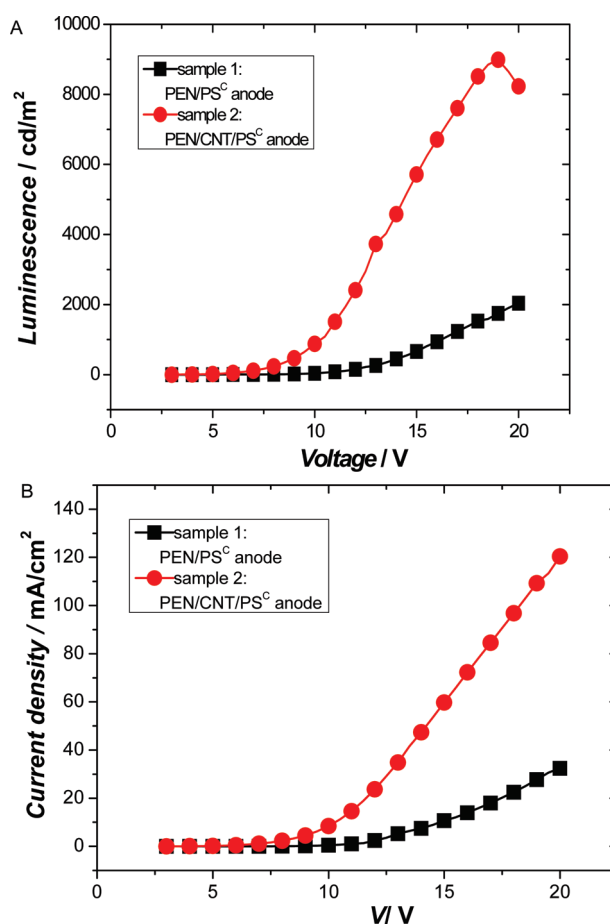


**Figure 2. Response characteristics of OLEDs built on PEN/PEDOT:PSS composite (sample 1) and vs PEN/CNT/PEDOT:PSS composite layer (sample 2): (A) luminescence vs voltage, (B) current density vs voltage.**

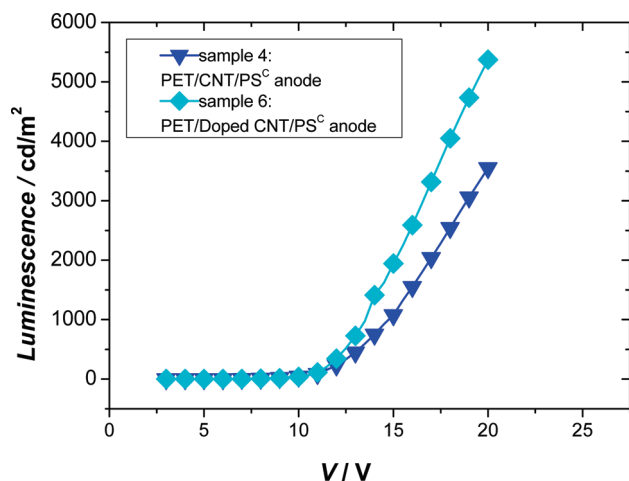


**Figure 3.** Luminescence vs voltage of OLEDs for PET/CNT/PEDOT:PSS composite (sample 4) vs PET/doped CNT/PEDOT:PSS composite (sample 6).

Five nm polymer was used to improve the adhesion of CNT thin films onto PET or PEN substrate for better handling and device fabrication process. However, such a thin layer of material as modification for transparent CNT thin film may have a negative effect on the OLED device performance since such a layer could po-

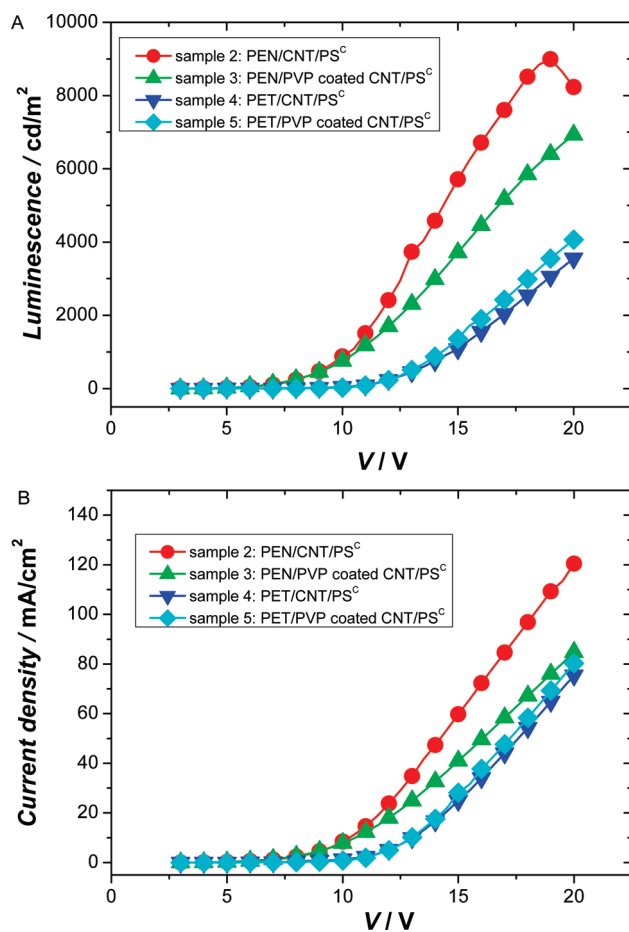


**Figure 4.** Response characteristics of OLEDs to compare between CNT samples with and without polymer top coating (refer to Table 1 for exact description of samples 2, 3, 4, and 5): (A) luminescence vs voltage, (B) current density vs voltage.

tentially inhibit the charge injection from the electrodes to the active layer, resulting in poorer device performance. Figure 4 shows the comparison for devices with or without polymer top coating as adhesion improvement. It also compares devices built on PET and PEN substrates. The devices built on PEN substrates (samples 2 and 3) show better performance than the devices built on PET substrates (sample 4 and 5). The molecular structure of PEN consists of two aromatic rings while PET only contains one aromatic ring.<sup>30</sup> As a result, the greater delocalized  $\pi$  electron cloud in PEN from two aromatic rings would most likely promote greater CNT adhesion and parallel alignment to the PEN surface than compared to PET, thus influencing the sheet resistance of CNT deposited on PEN and PET (Table 4). The lower sheet resistance of sample 2 explains why its performance is better than sample 4. Further comparison shows that the devices built on PEN substrates with top polymer coating (sample 3) show worse performance than that without polymer coating (sample 2), but the devices built on PET substrates with top polymer coating (sample 5) show better performance than that without (sample 4). These results may require further study and analysis. However OLED performance appears primarily to be determined by the sheet resistance of the modified CNT anode; the sheet resistance values in Table 1 show that the devices with better performance have lower sheet resistance. It is very likely that the sheet resistance is the most critical parameter in dictating the OLED devices performance once the minimum requirements for roughness and work function have been met. Further study shows that there is no shift in turn-on voltage after polymer top coating. For commercialization of CNT thin films as anode, good adhesion is required. Another method to improve the adhesion is to use a promotion layer which is put under CNT thin films, not on top. For OLED applications, a promotion layer rather than top coating polymer may be preferred if the top coating materials have an inherent insulating nature. Conductive polymers are another choice as top coating materials, but the instability and other problems of conductive polymers make them less attractive.

Another promising phenomenon we observed is that the relatively stable efficiency values were maintained over the voltage range of 4–20 V for the PEN samples and 11–16 V for the PET samples. Figure 5 shows an example of the stable efficiency. The maximum efficiency values of PEN/CNT/PS<sup>c</sup> (10.7 cd/A, 102.9  $\Omega$ /sq), PEN/CNT/5 nm polymer/PS<sup>c</sup> (9.3 cd/A, 116.1  $\Omega$ /sq), PET/Doped CNT/PS<sup>c</sup> (8.2 cd/A, 135.5  $\Omega$ /sq), and PET/CNT/5 nm polymer/PS<sup>c</sup> (6 cd/A, 150.2  $\Omega$ /sq) are similar to OLED devices using an ITO anode and C545-doped emissive layers (4.5 cd/A).<sup>31,32</sup> This can be attributed to a better balance of holes and electrons in the recombination zone when the current density was increased.

We have developed a simple method for the fabrication of high performance flexible OLED devices using CNT as the anode after surface modification. The ability to modify the work function of CNT using  $\text{HNO}_3$  doping and PEDOT:PSS composite ( $\text{PSC}$ ) solution could prove important in the development of using CNT films for other applications that require a range of work functions. Impressive OLED luminescence, current density, and efficiency were achieved incorporating  $\text{PSC}$  layer and CNT anode. The next step would be to explore various methods and materials to bring it up to the stringent requirements of an OLED device that has long lifetime ( $>50000$  h), high power efficiency, and high cost competitiveness in order to break into the flexible display market within the next decade. The device performance improvement after the modification on CNT anodes indicates there is great potential to further improve OLED performance by using CNT thin film anode in OLED devices. Transparent TCO electrode have been studied and continuously improved for the last few decades. In the future, more efforts will also be seen for transparent CNT thin film electrode and modification with other materials to lower the work function suitably

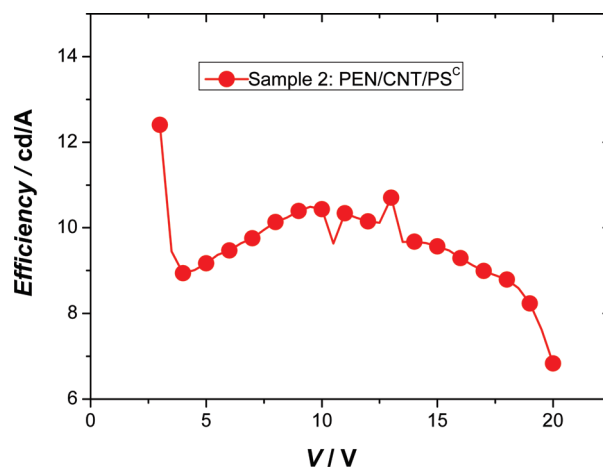


Figure 5. Efficiency of OLED device (sample 2) PEN/CNT/ $\text{PSC}$  which shows stable efficiency in a broad voltage range.

for use as a cathode layer, to realize transparent displays with CNT anode and cathode. Combined with CNT thin film superior mechanical flexibility, flexible OLED display with CNT thin film electrodes is one of the most promising combinations.

## EXPERIMENTAL SECTION

CNT thin films on PEN and PET substrates were fabricated with the high speed roll-to-roll slot die method. Carbon nanotubes were dispersed in water with the aid of surfactant. Coating aids were used for tuning the rheology and coatibility on selected substrates. The conductivity is calculated using the formula in our previous publication.<sup>33</sup> The resistance was measured using a 4 pin probe model from Mitsubishi Chemicals, and roughness was measured using atomic force microscopy. CNT films on PET substrates were subsequently subjected to a 10 min 8 M  $\text{HNO}_3$  acid soaking which reduced the sheet resistance, dropping from 282.0 to 141.1  $\Omega/\text{sq}$  (sample 6). To improve the adhesion between nanotube thin films and substrate, 5 nm thick of PVP polymer-coated with Meyer rod method was used to encapsulate CNT films. The  $\text{PSC}$  solution was filtered with a 0.45  $\mu\text{m}$  polyvinylidene difluoride (PVDF) syringe filter and subjected to ultrasound for 10 min. The CNT films on PEN substrates and doped/undoped CNT films on PET substrates were then treated with ozone plasma for 3 s before spin coating with the  $\text{PSC}$  at 600 rpm for 90 s and 2000 rpm for 30 s before baking at 120  $^\circ\text{C}$  for 2 h under an  $\text{N}_2$  environment. Ozone plasma treatment surface functionalizes the CNT surface by forming carboxylic groups.  $\text{PSC}$  contains polyethylene glycol (PEG) additive in Baytron P500 which helps increase the conductivity of the PEDOT:PSS. In addition, the PEG has numerous ether groups containing oxygen in between the terminal hydroxyl groups. When the  $\text{PSC}$ , containing free ungrafted PEG additive, is spin coated onto the CNT functionalized with  $\text{C}=\text{O}$  groups, the hydroxyl groups on these free ungrafted PEG molecules react with the carboxylic groups on the CNT walls. This causes the PEG to be grafted onto the ozone-functionalized CNT. During the spin coating of  $\text{PSC}$  onto ozone treated CNT, the PEG-PEDOT:PSS are bonded to the CNT walls through hydrogen bonding of the ether groups of grafted PEG and terminal hydroxyl groups of the free ungrafted PEG.

The sheet resistance and roughness of the films were measured again after coating with  $\text{PSC}$  solution.  $\text{PSC}$  solution was also spin coated onto bare plastic PEN substrates to evaluate the actual sheet resistance and roughness of the spin-coated film. Bending test was performed on the  $\text{PSC}$ -coated PEN and PET samples as well as the original samples to determine the bending resistance of the samples. The samples were subjected

to 10000 cycles bending with curvature radius of 12.5 mm and frequency of one cycle per second. UPS measurements were carried out in an XPS-ESCA LAB-220i XL (VG Scientific) equipment to determine the work function of the original CNT films as well as the  $\text{PSC}$ -coated CNT films. The luminescence measurement were captured in a nitrogen filled glovebox using a Konica Minolta chroma meter CS-200 and Keithly source meter 2420 and data were recorded by Labview. A 4-diode device with dimension of  $5 \times 5$  cm was fabricated using CNT films coated onto the PEN and PET substrates. A positive photoresist AZ 4620 was spin-coated onto the  $\text{PSC}$  layer and after developing; the samples were subjected to  $\text{O}_2$  reactive ion etching (RIE) to pattern  $\text{PSC}$ -modified CNT film. The sheet resistance of the  $\text{PSC}$ /CNT films remained the same after the patterning. The device was eventually completed using a stack of small molecule organic layers and metal cathode using high vacuum deposition in an Ulvac thermal evaporator. The organic stack consists of a 75 nm  $N,N'$ -diphenyl-1,1-bihyl-4,4-diamine (NPB) and a 75 nm tris-(8-hydroxyquinoline) aluminum ( $\text{Alq}_3$ ) coevaporated with coumarin 545. The cathode layer consists of 0.5 nm lithium fluoride, 20 nm calcium, and 100 nm silver after the organic layer deposition.

*Acknowledgment.* Funding support to evaluate CNT for OLEDs and OLED fabrication from IMRE core project IMRE/06-1R0140 is acknowledged.

## REFERENCES AND NOTES

- Iijima, S. Helical Microtubules of Graphitic Carbon. *Nature* **1991**, *354*, 56–58.
- Thostenson, E. T.; Li, C.; Chou, T. W. Nanocomposites in Context. *Compos. Sci. Technol.* **2005**, *65*, 491–516.
- Kilbride, B. E.; Coleman, J. N.; Fraysse, J.; Fournet, P.; Cadek, M.; Drury, A.; Hutzler, S.; Roth, S.; Blau, W. J. Experimental Observation of Scaling Laws for Alternating Current and Direct Current Conductivity in Polymer–Carbon Nanotube Composite Thin Films. *J. Appl. Phys.* **2002**, *22*, 4024–4030.
- Moon, J. S.; Park, J. H.; Lee, T. Y.; Kim, Y. W.; Yoo, J. B.; Park, C.; Kim, J. M.; Jin, K. W. Transparent Conductive Film Based on Carbon Nanotubes and PEDOT Composites. *Diamond Relat. Mater.* **2005**, *14*, 1882–1887.

5. C.M Aguirre, C. M.; Auvray, S.; Pigeon, R. S.; Izquierdo, P.; Desjardins, R. Martel. Carbon Nanotube Sheets as Electrodes in Organic Light-Emitting Diodes. *Appl. Phys. Lett.* **2006**, *88*, 183104-1–183104-3.
6. Zhang, D.; Koungmin, R.; Liu, X.; Polikarpov, E.; James, Ly.; Mark, E. T.; Zhou, C. Transparent, Conductive, and Flexible Carbon Nanotube Films and Their Application in Organic Light-Emitting Diodes. *Nano. Lett.* **2006**, *6*, 1880–1886.
7. Fournet, P.; Coleman, J. N.; Lahr, B.; Drury, A.; Blau, W. J.; O'Brien, D. F.; Hörhold, H. H. Enhanced Brightness in Organic Light-Emitting Diodes Using a Carbon Nanotube Composite as an Electron-Transport Layer. *J. Appl. Phys.* **2001**, *90*, 969–975.
8. Landi, B.; Raffaele, R.; Castro, S.; Bailey, S. Single-Wall Carbon Nanotube-Polymer Solar Cells. *Prog. Photovolt: Res. Appl.* **2005**, *13*, 165–172.
9. Du Pasquier, A.; Unalan, H. E.; Kanwal, A.; Miller, S.; Chhowalla, M. Conducting and Transparent Single-Wall Carbon Nanotube Electrodes for Polymer–Fullerene Solar Cells. *Appl. Phys. Lett.* **2005**, *87*, 203511–1203511–3.
10. Khabashesku, V. N.; Margrave, J. L.; Barrera, E. V. Functionalized Carbon Nanotubes and Nanodiamonds for Engineering and Biomedical Applications. *Diamond Relat. Mater.* **2005**, *14*, 859–866.
11. Spinks, G. M.; Mottaghitalab, M. V.; Bahrami, S. P. G.; Whitten, G.; Wallace, G. Carbon-Nanotube-Reinforced Polyaniline Fibers for High-Strength Artificial Muscles. *Adv. Mater.* **2006**, *18*, 637–640.
12. Lau, K. T.; Hui, D. Effectiveness of Using Carbon Nanotubes as Nano-Reinforcements for Advanced Composite Structures. *Carbon*, **2002**, *40*, 1605–1606.
13. Li, J.; Lei, W.; Zhang, X. B.; Zhou, X. D.; Wang, Q. L.; Zhang, Y. N.; Wang, B. P. Field Emission Characteristic of Screen-Printed Carbon Nanotube Cathode. *Appl. Surf. Sci.* **2003**, *220*, 96–104.
14. Gruner, G. Carbon Nanotube Films for Transparent and Plastic Electronics. *J. Mater. Chem.* **2006**, *16*, 3533–3539.
15. Zhang, M.; Atkinson, K. R.; Baughman, R. H. Multifunctional Carbon Nanotube Yarns by Downsizing an Ancient Technology. *Science* **2004**, *306*, 1358–1361.
16. Bower, C.; Zhou, O.; Zhu, W.; Werder, D. J.; Jin, S. Nucleation and Growth of Carbon Nanotubes by Microwave Plasma Chemical Vapor Deposition. *Appl. Phys. Lett.* **2000**, *77*, 2767–2769.
17. Huang, Z. P.; Xu, J. W.; Ren, Z. F.; Wang, J. H.; Siegal, M. P.; Provencio, P. N. Growth of Highly Oriented Carbon Nanotubes by Plasma-Enhanced Hot Filament Chemical Vapor Deposition. *Appl. Phys. Lett.* **1998**, *73*, 3845–3847.
18. Suzuki, S.; Bower, C.; Watanabe, Y.; Zhou, O. Work Functions and Valence Band States of Pristine and Cs-Intercalated Single-Walled Carbon Nanotube Bundles. *Appl. Phys. Lett.* **2000**, *76*, 4007–4009.
19. Zhao, J.; Han, J.; Lu, J. P. Work Functions of Pristine and Alkali-Metal Intercalated Carbon Nanotubes and Bundles. *Phys. Rev. B* **2002**, *65*, 193401-1–193401-4.
20. Michael, W. R.; Mark, A. T.; Michael, D. M. H-J. P.; Dennler, G.; Niyazi, S. S.; Hu, L.; Gruner, G. Organic Solar Cells with Carbon Nanotube Network Electrodes. *Appl. Phys. Lett.* **2006**, *88*, 233506-1–233506-3.
21. Tero, M.; Krisztian, K.; Sami, S.; Geza, T.; Jari, S. P.; Panu, H.; Heikki, S. Heli, Inkjet Printing of Transparent and Conductive Patterns of Single-Walled Carbon Nanotubes and PEDOT-PSS Composites. *Phys. Status Solidi B* **2007**, *244*, 4336–4340.
22. Li, J. F.; Hu, L.; Wang, L.; Zhou, Y.; Gruner, G.; Marks, J. T. Organic Light-Emitting Diodes Having Carbon Nanotube Anodes. *Nano Lett.* **2006**, *6*, 2472–2477.
23. Bhavin, E. P.; Giovanni, F.; Goki, E.; Manish, C. Improved Conductivity of Transparent Single-Wall Carbon Nanotube Thin Films via Stable Post-deposition Functionalization. *Appl. Phys. Lett.* **2007**, *90*, 121913–1121913–3.
24. Hu, L.; Hecht, D. S.; Gruner, G. Percolation in Transparent and Conducting Carbon Nanotube Networks. *Nano Lett.* **2004**, *4*, 2513–2517.
25. Wang, G. F.; Tao, X. M.; Wang, R. X. Flexible Organic Light-Emitting Diodes with a Polymeric Nanocomposite Anode. *Nanotechnology* **2008**, *19*, 145201–145205.
26. Jackson, R.; Domercq, B.; Jain, R.; Kippelen, B.; Graham, S. Stability of Doped Transparent Carbon Nanotube Electrodes. *Adv. Funct. Mater.* **2008**, *18*, 2548–2554.
27. Liu, P.; Sun, Q.; Zhu, F.; Liu, K.; Jiang, K.; Liu, L.; Li, Q.; Fan, S. Measuring the Work Function of Carbon Nanotubes with Thermionic Method. *Nano Lett.* **2008**, *8*, 647–651.
28. Li, J.; Hu, L.; Liu, J.; Wang, L.; Marks, T. J.; Grüner, G. Indium Tin Oxide Modified Transparent Nanotube Thin Films as Effective Anodes for Flexible Organic Light-Emitting Diodes. *Appl. Phys. Lett.* **2008**, *93*, 083306-1–803306-3.
29. Geng, H. Z.; Kim, K. K.; So, K. P.; Lee, Y. S.; Chang, Y.; Lee, Y. H. Effect of Acid Treatment on Carbon Nanotube-Based Flexible Transparent Conducting Films. *J. Am. Chem. Soc.* **2007**, *129*, 7758–7759.
30. Urszula, D. W.; Viera, S.; Ralf, G.; Jhang, S. H.; Kim, B. H.; Lee, H. J.; Ley, L.; Park, Y. W.; Berber, S.; David, T.; Roth, S. Effect of SOCl<sub>2</sub> Treatment on Electrical and Mechanical Properties of Single-Wall Carbon Nanotube Networks. *J. Am. Chem. Soc.* **2005**, *127*, 5125–5131.
31. Lechat, C.; Bunsell, A. R.; Davies, P.; Piant, A. Mechanical Behaviour of Polyethylene Terephthalate & Polyethylene Naphthalate Fibres under Cyclic Loading. *J. Mater. Sci.* **2006**, *41*, 1745–1756.
32. Hung, L. S.; Chen, C. H. Recent Progress of Molecular Organic Electroluminescent Materials and Devices. *Mater. Sci. Eng.* **2002**, *39*, 143–222.
33. Jay, L.; Sonia, G.; Babu, C.; Erik, V.; Dorota, T. Highly Flexible Transparent Electrodes for Organic Light-Emitting Diode-Based Displays. *Appl. Phys. Lett.* **2004**, *85*, 3450–3452.